EFFECT OF CORROSION ON THE PERMEABILITY OF HIGH-ALUMINA REFRACTORIES

Emmanuel de Bilbao[1], Séverine Brassamin [1], Jacques Poirier[1], Lise Loison [2], Thorsten Tonnesen[2]

[1] CNRS, CEMHTI UPR3079, Univ. Orléans, Orléans, France
[2] RWTH Aachen University, Institute of Mineral Engineering, Aachen, Germany

ABSTRACT

This work aimed at studying the effect of alumina Low Cement Castables corrosion on permeability. The objectives were:

i) To demonstrate the reliability of the new permeameter and the possibility to measure accurately the permeability.

ii) To evaluate the effect of the corrosion on the permeability of the refractory.

The corrosion tests were performed with basic and acidic slags coming respectively from steel and energy production (waste ashes). Scanning Electron Microscope and open porosity measurements complemented the permeability measurements. Finally the changes in microstructure and the permeability could be correlated.

INTRODUCTION

Permeability is a very important property of refractory materials. For example, it plays a key role in the dewatering of refractory castable [1], or in the resistance of refractory linings to the penetration of corrosive fluids [2]. For example, the corrosion of high-alumina refractory bricks and alumina-magnesia in situ spinel castables used in steel ladles by slag involves reactive impregnation where the slag impregnation is driven by the capillary suction and limited by the liquid permeability. The reaction of the slag with matrix and/or the grains of the refractory make the slag change in composition and the porous network as well. The slag viscosity and the corroded refractory permeability change subsequently, therefore modifying the reactions and the impregnation.

The objective of this work was to evaluate the permeability of refractory materials using the method suggested by standards ISO 8841:1991, DIN EN 993-4, and ASTM C577- 7 [3] using a standard permeameter.

However, standard methods do not allow to correctly determine the permeability and alternative approaches were used. In addition, an improved gas permeameter has been then developed to perform more accurate gas permeability measurements. The comparison between the results obtained with the two methods was done on a non-corroded alumina LCC refractory.

Then the permeability was measured on corroded part of sample to evaluate the effect of the corrosion.

PERMEABILITY MEASUREMENT

Intrinsic permeability is the property inherent to the material relating the pressure drop to the flow rate according the Darcy law. Different techniques have been developed to measure it: with gas or liquid and in unsteady state or steady state conditions. Gas permeability measurement in steady state conditions is the technique used in standards ISO 8841:1991 [3], DIN EN 993-4, and ASTM C577- 7 [4]. It consists in measuring the inlet pressure Pi, the outlet pressure Po, and the volumetric flow rate Q of the gas flowing through the sample and to derive the permeability parameters.

The integrated form of gas flow equation applied to the test in steady-state conditions depends on the flow regime. According to Forchheimer, its general form writes [5]:

$$\frac{{P_i}^2-{P_o}^2}{2PL} = \frac{\mu}{k_1} v + \frac{\rho}{k_2} v^2 \qquad (1)$$

where L is the sample thickness. Contrary to the standards, the pressure drop is expressed in function of the squared pressure due to the gas compressibility. The gas velocity v, or flow rate, varies from the entrance to the exit because of the pressure gradient and the gas compressibility. P is the absolute gas pressure for which the flow rate v is evaluated, that is P_i or P_o for v_i or v_o respectively. v is derived from the volumetric flow rate Q per cross-sectional area of the sample perpendicular to the flow. The dynamic viscosity of the gas μ is assumed to be constant within the applied pressure range. k_1 is Forchheimer viscous permeability. The second right-hand side term of the equation accounts for inertial effects due to dissipation of inertial energy as fluid particles accelerate through smaller pore throats and decelerate through larger area [6]. Although k_2 has the dimension of a length, it is called the non-Darcian or inertial permeability. When the flow rate is low, the inertia term vanishes and equation 1 becomes the Darcy equation applied to gas. k_1 is then the Darcean permeability.

According to Klinkenberg, the gas-slippage at pores wall leads to a pressure dependent permeability larger than that would be measured with liquid [7]:

$$k_a = k_\infty \left(1 + \frac{b}{P_m}\right) \qquad (2)$$

where k_a is the experimental apparent permeability:

$$k_\mathrm{a} = \frac{2PL\mu}{{P_i}^2-{P_o}^2} v \qquad (3)$$

k_∞ is called the intrinsic permeability and is expected to be the permeability one would measure with liquid. The slippage factor b accounts for the slippage of gas molecules and depends on both the molecular mean free path and characteristic length of pore geometry. P_m is the mean pressure of P_i and P_o.

The standards mentioned above recommend permeability measurement in atmospheric mode, for which the exit is left at atmospheric pressure and the gas leaving the sample is thereby allowed to flow directly at this pressure. The flow rate is measured at the outlet of the sample and $P = P_o$ in equation 1. In addition it is assumed that the mean pressure equals 1 atm. as the pressure drop is very small. However, the methods proposed by the standards do not allow for determining the intrinsic permeability and the slippage factor. It is possible to extend the standard method by applying increasing inlet pressure to get different sets of triplet (Pi, Po, v_o). The determination of the parameters starts by plotting the pressure drop function, which is the left-hand side of equation (1), versus the flow rate and fitting a linear or parabolic function giving the best correlation. The intrinsic permeability is then derived in two different ways depending on the shape of the fit:

i) If the best fit shows a linear shape, Darcean flow is assumed. The apparent permeability is calculated for each triplet according to the equation 3 and the Klinkenberg parameters, k_∞ and b, are determined, according to equation 2, by plotting apparent permeability versus the inverse mean pressure.

ii) If the best fit is quadratic, the Forchheimer parameters k_a and k_2 are derived. Assuming the mean pressure involved in inertial flow is high enough, the intrinsic permeability is equal to the

Darcean permeability of Forchheimer's equation: $k_\infty = k_1$. On the other hand, Innocentini et al. proposed to explain the pressure dependence of the apparent permeability by inertia rather than slippage effects. The authors proposed to calculate the experimental apparent permeability from k_1 and the Forchheimer's number F_o, which depends on the flow rate measured for each triplet (P_i, P_o, v_o):

$$k_a = \frac{k_1}{1+F_o} \quad (4)$$

Plotting the experimental apparent permeability versus the inverse mean pressure allowed for the determination of the intrinsic permeability.

In practice, the flow regime is not so easy to define because it can change from viscous to inertial as the flow rate increases. In addition, the flow rate may decrease significantly over the length of the sample in atmospheric mode due to the compressibility of gas. The best way to identify the intrinsic permeability is then to ensure the viscous flow regime by applying a backpressure to the sample ($P_o > P_{atm}$) and increasing progressively both inlet and outlet pressures. The pressure drop function plot allows for checking the viscous flow regime and Klinkenberg plot allows for identifying the intrinsic permeability and the slippage factor. An improved gas permeameter has been then developed. It includes a mass flow controller put at the inlet to control the flow regime and valves put at the outlet to apply a backpressure if needed.

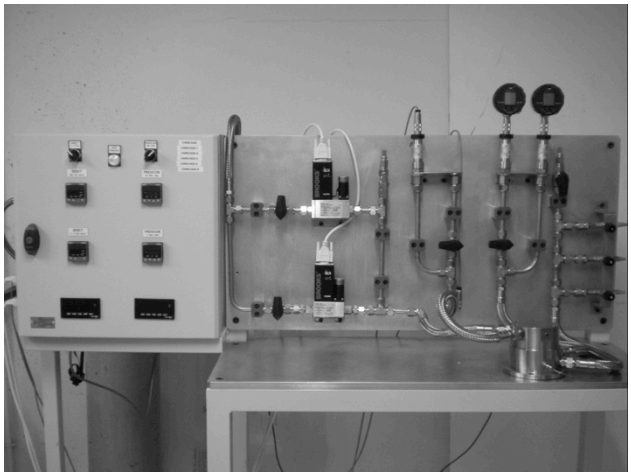

Fig. 1: Permeability measurement device with two inlet mass flow controllers and 3 back pressure control valves.

MATERIALS AND EXPERIMENTS

Refractory Materials

Samples of low cement castables (LCC) were produced to test the relevance of permeability measurement on refractory products. The composition of the test castable is summed up in Tab. 1. All high alumina raw materials, sintered Al_2O_3, have been provided by Alteo. The cement used in the composition was supplied by Kerneos. The citric acid as retarder and the deflocculant supplied by BASF were dissolved in water to complete the formulation of the Low Cement Castable. The castable was cast in cylindric mould of D50 mm x H 50mm.The samples were then cured for 48 h in a humid environment, dried for 24 h and sintered at 1500 °C for 6 hours, prior to polishing and cutting. Open porosity, bulk density, and weight were evaluated for each sample. The mean open porosity was 17.9 %. The mean bulk density was 3.04 g/cm^3.

Tab. 1: Composition of the alumina LCC

	Raw material	Weight %
Matrix	CA Cement	5.0
	Reactive Alumina / PFR	12.5
Aggregates	Tabular Alumina / 0-3 mm	82.5
	Water	5.0
Additives	Deflocculant	0.20
	Retarder	0.03

Slag

The corrosion tests were performed with industrial slags coming respectively from energy and steel production (Tab. 2 and Tab. 3). The melting temperatures, assessed by hot-stage microscopy, were of 1190 °C and 1346 °C for waste slag and steel slag, respectively. Pellets of 5 g and 15 g were prepared with each slag.

Tab. 2: Composition of waste slag (wt.%)

SiO_2	Al_2O_3	FeO_3	CaO	MgO	K_2O	Na_2O	P_2O_5	L.O.I
45.4	13.7	4.9	23.3	2.6	0.9	2.4	2.8	4

Tab. 3: Composition of steel slag (wt.%)

SiO_2	Al_2O_3	FeO_3	CaO	MgO	K_2O	Na_2O	TiO_2	MnO
32.3	10.1	0.3	47.0	5.5	0.5	0.2	1.1	0.4
ZrO_2	SO_3							
0.04	2.55							

Corrosion tests

The corrosion test consisted in placing the cylindrical samples into a furnace with a pellet of slag on top. The samples were heated to 1500 °C in air with a rate of 2 °C/min. After a 70-hour dwell, the sample were cooled with a rate of 2 °C/min. Each sample was cut into 4 disks of about 10 mm thick and the permeability was measured for each disk. The measurements were carried out according to the standard ISO 8841:1991, which is equivalent to DIN EN 993-4, by letting the outlet at atmospheric pressure (Fig. 2).
Finally, the microstructure of corroded sample was examined by scanning electron microscopy.

Fig. 2: Permeability measurement device according to DIN EN 993-4

RESULTS

Permeability measurement of not corroded LCC

First, the permeability of an alumina LCC sample was measured by using a permeameter based on the DIN standard. The sample was 35 mm in diameter and 10 mm in height. The gas was dry

air (μ=1.81×10^{-5} Pa.s at 20 °C) and the exit was kept at atmospheric pressure. The outlet volumetric flow rate ranged from 7×10^{-4} up to 32×10^{-4} m/s while the inlet pressure ranged from 0.153 up to 0.235 MPa.

Figure 3 shows the pressure drop function. Both linear and quadratic regressions have been calculated to fit the experimental data. The negative coefficient of the quadratic curve indicates that the flow remained viscous over the test.

Figure 4 shows the Klinkenberg plot where the apparent permeability calculated for each triplet is plotted versus the inverse mean pressure according to equation 2. The intrinsic permeability derived from the fitting line is 2.37×10^{-15} m^2.

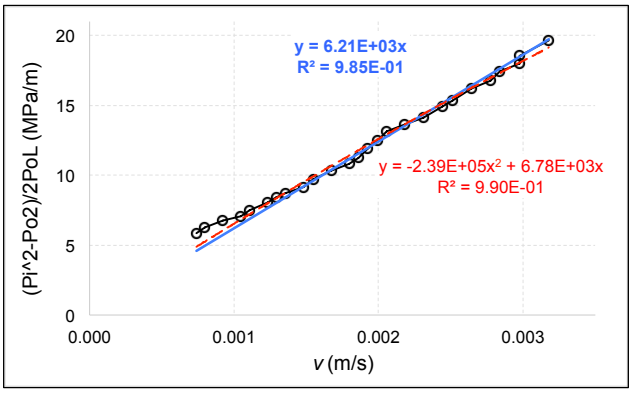

Fig. 3: Pressure drop function plot for Alumina LCC. The negative coefficient of the quadratic regression indicates that the flow remained viscous during the test.

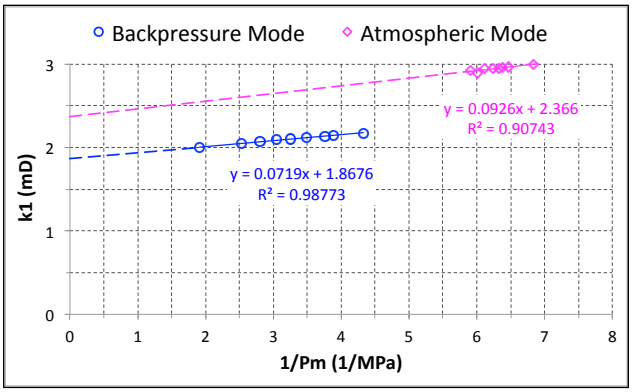

Fig. 4: Klinkenberg plot for Alumina LCC. Diamonds represent the results of measurements in atmospheric mode according to DIN standard. Positive slope of the linear regression shows Klinkenberg effect. However, measuring points closer to the zero inverse mean pressure could increase the accuracy of the fitted parameters. Circles represent the results of measurements in backpressure mode with constant mas flow rate control. Backpressure allows for reaching lower inverse mean pressure and therefore more accurate evaluation of intrinsic permeability.

Second, the permeability of the same sample was also measured with the improved permeameter, which allows for performing test at low constant mass flow rate with backpressure. The sample was 35 mm in diameter and 40 mm in height. The gas was Nitrogen (μ=1.76×10^{-5} Pa.s at 20 °C). The equivalent volumetric flow rate at normal condition was 0.14 NL/min. The inlet and outlet pressure ranged from 0.415 up to 0.607 MPa and from 0.100 up to 0.440 MPa. The intrinsic permeability derived from the Klinkenberg plot is 1.87×10^{-15} m^2 (Fig. 4). Considering the difference between the two devices and the difference between the two samples, one can estimate this value close to the one obtained in the first measurement.

Corrosion of LCC by waste slag

A thin crust formed on the top of the LCC samples corroded with waste ash (fig. 5, left). Previous crucible tests showed that the waste slag penetrated the LLC crucible and reacted with the matrix to form a liquid phase at high temperature as suggested by the round porosity and the glassy aspect of the crust [8]. The micrograph (fig. 6) shows that the slag attacked more the matrix rather than the grains that have not been much degraded. Below the crust, the slag filled the porous space.

Fig. 5: Corroded samples with 15 g of waste slag (left) and 5 g of steel slag (right). 1550 °C for 70 hrs.

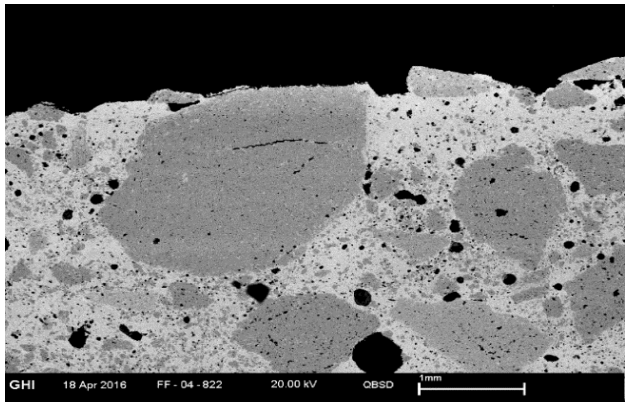

Fig. 6: LCC corroded by waste slag

Tab. 4 summarises the open porosity and the intrinsic permeability measured on the cut disks. Position 1 corresponds to the top of the sample. The open porosity clearly indicates that the positions 3 and 4 have not been corroded for both samples. The difference between the non-corroded parts of the samples (17.5 % vs 12 %) may be due to the reproducibility in sample making. The open porosity of the LCC sample corroded with 5 g of waste slag decreased from 17.5 % down to 9 % on the top. Note that the disk 1 includes both the thin crust and the corroded part with pores filled by the slag. In the case of sample corroded with 15 g of slag, the porosity is more homogeneous in disks 1 and 2. The area corresponding to disk 2 has been more infiltrated by the slag.

The permeability of the non-corroded part of the samples differs in agreement with the difference of the porosity. The porosity of disk 1 with 5 g of slag decreased drastically (0.07 mD). The permeability of disk 2 results from a corroded volume with very low value and a non-corroded volume with higher initial permeability. The evolution of the permeability of the sample corroded with 15 g of slag is different as permeability of the disk 1 is higher than the one of disk 2. It could be explained by the fact that if porosity is equal in the both disk, the pore size distribution might be not the same. Pores in disk 1 could be

bigger than the ones in disk 2. This could explain the difference in slippage factor values, as well.

Tab. 4: Klinkenberg permeability after corrosion by waste slag

	Pos.	State	K_∞ (mD)	b (kPa)	Φ (%)
Waste slag 5 g	1	Corroded	0.07	1430	9.0
	2	Corroded	2.61	40	12.3
	3	Not corroded	6.11	0	17.4
	4	Not corroded	5.68	40	17.6
Waste slag 15 g	1	Corroded	1.47	250	7.0
	2	Corroded	0.08	750	6.5
	3	Not corroded	3.00	10	13.3
	4	Not corroded	1.72	50	11.0

Corrosion of LCC by steel slag

The top of the samples corroded by steel slag differs from the ones corroded by waste slag (Fig. 5). The slag penetrated deeper the LLC sample without forming a crust. The infiltration depth of the slag macroscopically visible and is around 10 mm with 5 g of steel slag and 17 mm with 15 g. Contrary to the results with waste slag, the porosity increased in the upper part of the samples (Tab. 5) due to the crack formation during the cooling of the sample as can be seen in Fig. 7. The porosity resulting from the corrosion test with 15 g in disk 2 is lower than the non-corroded part. This confirms that porosity increase is due the crack formation while corrosion by slag makes the porosity decrease. Porosity of disks 1 and 2 forth both amounts of slag is very well correlated with the depth of penetration. The permeability changes with the same trend of the porosity apart from disk 2 with a lower permeability should expected due to the pores clogging in this part.

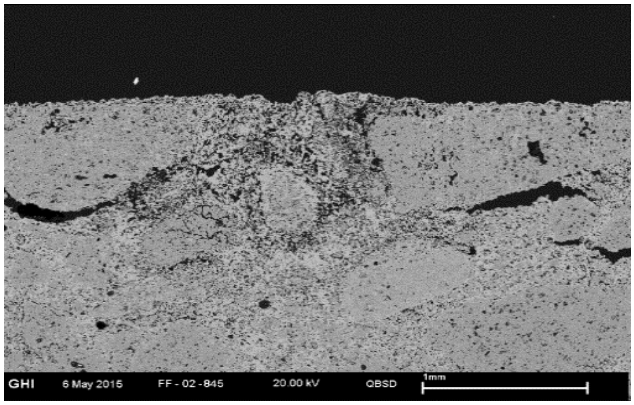

Fig. 7: LCC corroded by steel slag

Tab. 5: Klinkenberg permeability after corrosion by steel slag

	Pos.	State	K_∞ (mD)	b (kPa)	Φ (%)
Steel slag 5 g	1	Corroded	7.11	80	19.0
	2	Not corroded	4.49	70	17.9
	3	Not corroded	5.21	50	17.5
	4	Not corroded	4.92	30	15.6
Steel slag 15 g	1	Corroded	6.87	3320	23.7
	2	Corroded	5.65	20	13.5
	3	Not corroded	4.47	60	16.8
	4	Not corroded	4.01	60	17.4

CONCLUSION

Although standards of permeability measurement do not allow for identifying the intrinsic permeability, it is possible to have a reasonable estimation by improving the method. Permeameter with flow rate control and backpressure allows for accurate permeability measurement. Measures performed on sample made of alumina low cement castable showed that both permeability values were close.

The measurement of permeability on corroded and not corroded parts of sample after corrosion tests showed that the corrosion by acidic and basic slags made the permeability to decrease. The permeability decreased much more with acidic waste slag than with basic steel slag. Moreover, cracks induced by the cooling made the permeability to increase. Finally, the change in permeability was related to the change in porosity and microstructure.

REFERENCES

[1] da Luz AP, Braulio MAL, Pandolfelli VC. Refractory castable engineering. F.I.R.E. Compendium Series. Vol. 1. Baden-Baden: Göller Verlag GmbH. 752. 2015

[2] de Bilbao E, Poirier J, Bouchetou ML, Blond E. Modelling of reactive impregnation and phase transformations during the corrosion of high alumina refractories by Al2O3-CaO slag. In: Advances in Science and Technology, Vol. 92. CIMTEC 2014. Montecatini (Italy). 2014. p 264-271.

[3] Dense, shaped refractory products - Determination of permeability to gases, ISO 8884-91 8884-91, I.S. Organisation, 1991

[4] Standard Test Method for Permeability of Refractories, ASTM C577-07, ASTM, 2007

[5] Forchheimer P. Wasserbewegung durch boden, Zeit. Ver. Deutsch. Ing. 1901;**45** 1781-8.

[6] Rushing JA, Newsham KE, Lasswell PM, Cox JC, Blasingame TA. Klinkenerg-Corrected Permeability Measurements in Tight Gas Sands: Steady-State Versus Unsteady-State Techniques. Society of Petroleum Engineers. 2004.

[7] Klinkenberg LJ. The Permeability Of Porous Media To Liquids And Gases. In: API Drilling and Production Practice. American Petroleum Institute: Tulsa. 1941. p. 200-13.

[8] Telle R, Tonnensen T, Loison L, Sadou S. Correlation of the chemical composition of biomass slag with the post-mortem elastic propoerties of an alumina low cement castable after corrosion. In: 59th International Colloquium on Refractories. Aachen, Germany: ECREF. 2016. p68-71.